Microchimica Acta (2020) 187:550
https://doi.org/10.1007/s00604-020-04477-3

ORIGINAL PAPER

Flow injection enzymatic biosensor for aldehydes based on a Meldola Blue-Ni complex electrochemical mediator

Ana Maria Titoiu[1] · Georgiana Necula-Petrareanu[2] · Diana Visinescu[3] · Valentina Dinca[4] · Anca Bonciu[4,5] · Cristian N. Mihailescu[4] · Cristina Purcarea[2] · Rabah Boukherroub[6] · Sabine Szunerits[6] · Alina Vasilescu[1]

Received: 21 March 2020 / Accepted: 4 August 2020

Abstract

Carbon nanofibers (CNF) are efficient electrode modifiers in electrochemical biosensors that enhance the electrochemical active area, induce electrocatalytic effect toward the oxidation of the enzymatic cofactor nicotinamide adenine dinucleotide (reduced form, NADH), and enable the quantitative immobilization of enzymes. Combining CNF with efficient and stable mediators radically augments the speed of electron transfer between NADH and solid electrodes and leads to electrochemical sensors characterized by high sensitivity and stability. The main aim of this work was to investigate the performance of a novel mediator for NADH with advantageously low solubility in an electrochemical detector based on a screen-printed CNF electrode as well as its potential in biosensing. Using a mediator, prepared from Meldola Blue and Ni hexamine chloride, a stable and sensitive electrochemical NADH sensor is provided with a detection limit of 0.5 μmol L^{-1}. Further on, covalent immobilization of a recently described aldehyde dehydrogenase from the Antarctic *Flavobacterium PL002* strain on the surface of the mediator-modified electrode produced a stable biosensor for the detection of aldehydes. When integrated in a flow injection analysis (FIA) setup with amperometric detection at 0.1 V vs. Ag/AgCl, the measurement of benzaldehyde with a detection limit of 10 μmol L^{-1} over a linear range of 30–300 μmol L^{-1} is possible. Determination of trace benzaldehyde impurities in a pharmaceutical excipient was also demonstrated and results compared with a chromatographic method.

Keywords Carbon nanofibers · Electrochemical mediator · NADH · Aldehyde dehydrogenase · Flow injection analysis · Benzaldehyde sensing

Introduction

Many important biotransformations in biological systems and industrial processes use the enzymatic cofactor recycling system between nicotinamide adenine dinucleotide (NAD^+) and its reduced form NADH based on the following reaction:

$$Substrate + NAD^+ + H_2O \overset{dehydrogenase}{\rightarrow} Product + NADH + H^+ \quad (1)$$

Ana Maria Titoiu and Georgiana Necula-Petrareanu contributed equally to this work.

Electronic supplementary material The online version of this article (https://doi.org/10.1007/s00604-020-04477-3) contains supplementary material, which is available to authorized users.

✉ Alina Vasilescu
avasilescu@biodyn.ro

[1] International Centre of Biodynamics, 1B Intrarea Portocalelor, 060101 Bucharest, Romania

[2] Institute of Biology, 296 Splaiul Independentei, 060031 Bucharest, Romania

[3] Coordination and Supramolecular Chemistry Laboratory, "Ilie Murgulescu" Institute of Physical Chemistry, Romanian Academy, Splaiul Independentei 202, 060021 Bucharest, Romania

[4] National Institute for Laser, Plasma and Radiation Physics (INFLPR), 409 Atomistilor, 077125 Magurele, Romania

[5] Faculty of Physics, University of Bucharest, 077125 Magurele, Romania

[6] Univ. Lille, CNRS, Centrale Lille, Univ. Polytechnique Hauts-de-France, UMR 8520 - IEMN, F-59000 Lille, France

Published online: 05 September 2020

The detection of the substrate, according to the above transformation (1), is achieved via measuring the quantity of NADH formed in the enzymatic reaction. In NADH electrochemical sensors, surface modification with carbon nanomaterials allows for enhanced sensitivity and minimized fouling and reduces the overpotential for NADH oxidation by up to 0.45 V [1]. Among carbon nanomaterials with good mechanical and electrical properties, carbon nanofibers (CNF) are remarkable, owing to their large surface area and high density of functional groups facilitating the quantitative immobilization of biomolecules [2] and electrocatalytic effects toward the oxidation of various compounds, including NADH [3].

In a previous work, we have shown that screen-printed CNF electrodes have better electrocatalytic properties toward the detection of NADH compared with electrodes modified with graphene, single-wall carbon nanotubes, or mesoporous carbon [4], enabling a ~ 0.2 V cathodic shift in the oxidation potential of NADH. CNF electrodes strongly adsorbed Meldola Blue (8-dimethylamino-2,3-benzophenoxazine) and the obtained sensors provided higher catalytic currents for NADH and low capacitive current compared with the other three types of carbon nanomaterial–based electrodes [4]. These results align with other studies on MB-carbon nanomaterial electrode modifiers [5, 6], MB being one of the most efficient mediators, allowing for a dramatic, i.e. up to 0.8 V, decrease of the potential for NADH oxidation [7, 8] and being thus often preferred in biosensors based on dehydrogenases.

While due to its aromatic structure, MB is quantitatively adsorbed by π-π stacking on carbon nanomaterials such as CNT or CNF, its good solubility in water represents a serious limitation in sensing devices requiring long-term operational stability. Prevention of mediator leakage in sensors was attempted by (i) adsorption on oxides or phosphates and inclusion of the modified material in the carbon paste [9], (ii) inclusion in the screen-printing paste [10], (iii) attachment to thiols forming self-assembled monolayers [11], (iv) entrapment in polymers [12], (v) attachment by π-π stacking to carbon nanomaterials [5, 6], (vi) precipitation by complexation with Reinecke salt [13], (vii) electrodeposition of hybrid oxide/mediator films [14], (viii) electropolymerization [15] etc.

Progressing from our previous research [4] and in line with the above efforts to deliver NADH detectors with combined sensitivity and operational stability, we report the functionalization of screen-printed CNF electrodes with a novel, efficient MB-based mediator with low water solubility. The mediator was obtained by reacting MB with a complex of hexamine nickel (II) chloride, $[Ni(NH_3)_6]Cl_2$ (NiAm). Furthermore, to investigate the potential of modified electrodes to assist in the detection of NAD^+-dependent dehydrogenase substrates, a recently reported aldehyde dehydrogenase from the Antarctic microorganism *Flavobacterium PL002* (F-ALDH) was covalently attached to the electrode to form a stable biosensor. Aldehyde dehydrogenase (ALDH)–based biosensors provide simpler, faster, and cost-effective analytical alternatives compared with the standard chromatographic methods and with chemical sensors/sensor arrays for the detection of aldehydes in a series of applications relevant for air quality and for food and pharmaceutical industries [16–18]. F-ALDH has the potential to operate in a larger range of temperature compared with the mesophilic, commercially available enzyme from baker's yeast. Building from its utility for benzaldehyde detection, demonstrated with the free enzyme in solution [4], this study reports the first biosensor based on this new and promising enzyme.

The biosensor was integrated into a flow injection analysis (FIA) setup and applied for the detection of benzaldehyde in benzyl alcohol, an inactive ingredient used as a preservative in pharmaceutical products. Benzaldehyde is the major impurity in benzyl alcohol and its maximum admissible concentrations are set at 0.05% and 0.15% in benzyl alcohol for parenteral and non-parenteral use, respectively, according to the European Pharmacopoeia [19]. The electrochemical biosensor proposed here represents an advantageous alternative tool to the costly and resource-consuming gas chromatographic standard methods [19] for screening benzyl alcohol in the pharmaceutical field.

Materials and methods

Reagents and materials

Meldola Blue, β-nicotinamide adenine dinucleotide (NAD^+, purity > 98%), reduced β-nicotinamide adenine dinucleotide (NADH, purity > 98%), β-mercaptoethanol (purity > 99.0%), bovine serum albumin (BSA), tris(hydroxymethyl)aminomethane (TRIS), sodium phosphate dibasic and sodium phosphate monobasic, sodium hydroxide, sodium chloride, β-mercaptoethanol, benzyl alcohol, vanillin, trans-cinnamaldehyde, 4-hydroxy benzaldehyde, glutaraldehyde, butyraldehyde, 5-hydroxymethyl-2-furalaldehyde, and 4-fluoro-benzaldehyde were obtained from Merck, Germany. Acetone was from VWR Prolabo Chemicals, France. Benzaldehyde, 2-furalaldehyde, propionaldehyde, and acetic acid were provided by Acros Organics, Austria. Benzoic acid was from the Pharmaceutical Institute, Romania. Ethanol was from Atochim, Romania. The aldehyde dehydrogenase from the *Flavobacterium PL002* strain was obtained as a recombinant protein in *Escherichia coli* BL21(DE3) [20]. The *Flavobacterium PL002* strain was isolated from Antarctic sea water. The Michaelis-Menten constant $K_M = 0.145$ mmol L^{-1} was calculated at 25 °C, in 0.1 mol L^{-1} glycine/KOH buffer pH 9.5 with benzaldehyde as substrate and 1 mmol L^{-1} NAD^+ as cofactor (full

enzyme characterization to be reported in another paper). The enzyme was stored at − 20 °C with 20% glycerol.

The solutions used for the pH study were 0.1 M TRIS buffer solutions of pH 8.0, 8.5, 9.0, and 9.5 and 0.1 M phosphate buffer solutions of pH 7.4 and pH 10. All buffer solutions contained 0.1 M KCl.

Screen-printed 3-electrode systems were purchased from Metrohm Dropsens (Oviedo, Spain) and included a carbon counter electrode and a silver pseudo-reference electrode, in addition to the working electrode (4 mm in diameter) that was either carbon (DRP110) or carbon modified with nanofibers (DRP110D). Carbon electrodes modified with nickel oxide (DRP110 Ni) from the same producer were also used in some tests.

Preparation of Meldola Blue-Ni amine mediator and modified electrodes

The hexaammine nickel (II) chloride, $[Ni(NH_3)_6]Cl_2$, was prepared by using chloride salt of Ni(II) instead of nitrate salt according to [21]. The freshly prepared $[Ni(NH_3)_6]Cl_2$ complex, further on called NiAm, was kept at room temperature in the dark until use. A 5 mg mL^{-1} Meldola Blue was mixed in equal volumes with 6 mg mL^{-1} NiAm, and 6 μL of this mixture was deposited on the electrodes. After drying for 2 days at room temperature, the electrodes were rinsed copiously with water to wash any unbound material, dried under nitrogen, and kept at room temperature until use.

Immobilization of aldehyde dehydrogenase

A volume of 25 μL of 6.7 mg mL^{-1} F-ALDH (specific activity, 2 UI mg^{-1}) was mixed with 10 μL of 50 mg mL^{-1} BSA, 10 μL of 10 μM β-mercaptoethanol, and 5 μL of glutaraldehyde solution (1%). From this mixture, 6 μL was evenly spread on the surface of the working CNF/MB-NiAm electrode. After drying for 20 min at room temperature, the sensor was placed in the fridge and dried overnight. Next, the CNF/MB-NiAm/F-ALDH biosensor thus obtained was washed copiously with water, dried, and kept dry at 4 °C until use.

Flow injection analysis

Quantitative determination of NADH and benzaldehyde was achieved in a FIA setup in which the NADH sensor or aldehyde biosensor, respectively was used as an amperometric detector. The setup included a homemade flow-through electrochemical cell with a volume of 30 μL, connected to a 6-port manual injector with a sample loop of 190 μL, a peristaltic pump, and a VSP potentiostat (Princeton Applied Research, USA). A PC equipped with the EC Lab software was used to control the potentiostat and record the electrochemical signal. The modified electrodes (CNF/MB-NiAm for NADH detection or CNF/MB-NiAm/F-ALDH for benzaldehyde detection) were placed in the flow cell. For NADH analysis, PBS pH 7.4 was used as electrolyte and the working electrode was polarized at + 0.05 V vs. Ag/AgCl. For benzaldehyde analysis, the running buffer was 0.1 M phosphate buffer solution (pH 10) containing 0.1 M KCl and 10 μmol L^{-1} β-mercaptoethanol at a flow rate of 0.5 mL min^{-1} while the electrode was polarized at + 0.1 V vs. Ag/AgCl. Stock aldehyde and benzoic acid solutions (1 mol L^{-1}) were prepared in ethanol, while acetone and acetic acid stock solutions (1 mol L^{-1}) were prepared in water. All solutions were further diluted to the desired concentration with running buffer containing 1.75 mmol L^{-1} NAD^+ and then injected in the FIA system. Each sample was injected in triplicate. Spiked samples of benzyl alcohol were prepared by adding 9, 24, and 47 μL of the stock benzaldehyde solution per 1 mL of benzyl alcohol. For the analysis with the biosensor, the spiked samples were diluted 1:50 to 1:400 with NAD^+-containing buffer by serial dilutions, while the unspiked benzyl alcohol was diluted 1:50 with the same buffer. For these dilution factors, no deleterious effects were observed on enzyme activity due to benzyl alcohol. The concentration of benzaldehyde in benzyl alcohol samples was calculated based on the calibration curve.

Characterization methods

X-Ray photoelectron spectroscopy (XPS) was recorded using ESCALAB 220 XL spectrometer from Vacuum Generators featuring a monochromatic Al Kα X-ray source (1486.6 eV) and a spherical energy analyzer operated in the CAE (constant analyzer energy) mode (CAE = 100 eV for survey spectra and CAE = 40 eV for high-resolution spectra), using the electromagnetic lens mode. The angle between the incident X-rays and the analyzer is 58° and the detection angle of the photoelectrons is 30°.

Morphological investigations were carried out using a scanning electron microscope (JSM-531 Inspect S Electron Scanning Microscope, FEI Company) operating at 5–25 kV. Qualitative chemical evaluation of the samples was performed using energy-dispersive X-ray spectrometer (EDAX, Element 2CB detector on a JSM-531 Inspect S Electron Scanning Microscope, FEI Company), operated at 5 kV. The data were obtained from at least three different locations on each sample surface.

UV-vis absorption spectroscopy (Thermovision Evolution 600 spectrophotometer from Thermo Fischer Scientific) was performed to study the formation of MB-NiAm and to determine the enzymatic activity of aldehyde dehydrogenase. The enzymatic activity of ALDH was measured based on NADH formation at 340 nm, as previously described [4].

Fourier transform infrared (FTIR) spectra of $[Ni(NH_3)_6]Cl_2$, Meldola Blue, and product MB-NiAm were recorded on a FTIR Bruker Tensor V-37 spectrophotometer, using KBr pellets, in the frequency range 4000–400 cm^{-1}.

HPLC analysis of benzyl alcohol samples

The measurements were performed using a LC-Net II/ADC HPLC system from Jasco, equipped with a PU-2089 Plus pump, a MD-2018 Plus Photodiode Array Detector, a FP-2020 Plus FLD detector, and the ChromNav software. The analytical column was Kinetex C18, 250 × 4.6 mm, particle size = 5 μm, and 100 Å pore size from Phenomenex. The mobile phase was water:acetonitrile = 50:50 at a flow rate of 0.6 mL min^{-1}, the injection volume was 5 μL, and quantitative detection was performed at 210 nm. Calibration was performed in the range 5–100 μg mL^{-1} (47–942 μmol L^{-1}) benzaldehyde. The benzyl alcohol samples, whether unspiked or spiked with 9, 24, and 47 mmol L^{-1} benzaldehyde, were diluted 200 times with mobile phase prior to the analysis.

Results and discussion

Characterization of MB-NiAm complex

Formation of complexes such as Reineckates is well known to lower the solubility of MB without influencing its ability to mediate the electrocatalysis of NADH oxidation [13]. Motivated by this, we obtained a novel mediator by reacting MB with a complex of hexaammine nickel (II) chloride, $[Ni(NH_3)_6]Cl_2$ (NiAm). The formation of the new compound, MB-NiAm, was emphasized by UV-vis absorption spectra recorded for mixtures of MB and NiAm at various ratios (1:0.2 to 1:10). While MB presents an absorption maximum at 559 nm, upon mixing with NiAm, the peak at 559 nm diminishes and a new adsorption peak appears with a maximum at 674 nm (Fig. S1 in Supplementary information, SI).

The formed MB-NiAm compound was further characterized by EDAX and FTIR. The EDAX analysis unveiled C (37.7 ± 2.51 at.%) and O (49.0 ± 0.57 at.%) as main elements, along with Ni (5.8 ± 1.79 at.%) and low contents of Na (1.2 ± 0.72 at.%) and Cl (0.02 ± 0.2 at.%). From the analysis of the FTIR spectrum, MB-NiAm appears to be a complex of Ni(II) ion with MBH (i.e., the reduced form of MB): the absence of the vibration modes of N-H ($\upsilon_{N\text{-}H}$, from the starting nickel hexamine complex) and of C_{phenyl} = N group (from MB) as well as the red shift of the absorption bands attributed to $\upsilon(C\text{-}N)_{heterocycle}$ and $\upsilon(C\text{-}N\text{-}C)_{heterocycle}$ vibrations, to ca. 1510 cm^{-1} and ca. 1357 cm^{-1}, respectively, suggests the coordination of Ni(II) ions to the N-H group of MBH (see Fig. S2 and discussion in SI) [22].

Consequently, this data indicates a structure of MB-NiAm that lacks NH_3 as a coordination ligand, as proposed in Fig. 1.

Characterization of MB-NiAm modified electrodes

CNF-coated screen-printed electrodes were modified with MB-NiAm by drop-casting and were afterwards characterized by SEM, EDAX, XPS, and electrochemistry (Fig. 2).

SEM images at high magnification show that the overlapping carbon nanofibers form a 3-dimensional mesh-like structure at electrode surface (Fig. 2a), increasing the surface area and potentially affecting the diffusion of molecules. Previous characterization of the CNF electrodes revealed that the nanofibers were homogeneously distributed over the electrode surface and had a high number of edges to the external side with oxygen-containing groups involved in NADH electrooxidation catalysis [4]. Upon modification of the CNF electrodes with drop-casted MB-NiAm, the surface heterogeneity and roughness increased (Fig. 2b and Fig. S3 in SI). This potentially indicates a larger effective electrochemical surface area.

The XPS survey spectrum of CNF electrodes (Fig. 2c) exibits only signals from C1s (97.55 at.%) and O1s (2.45 at.%). Modification of the CNFs with MB-NiAm results in addition to C1s (75.76 at.%) and O1s (4.33 at.%), in signals from N1s (14.48 at.%), Ni2p (1.81 at.%), and Cl2p (3.62 at.%) in agreement with the chemical composition of the electrode surface. The aromatic structure of MB enables efficient adsorption on carbon nanofibers via π-π stacking. Moreover, electrostatic interactions between the positively charged mediator and the negatively charged carbon fiber interface are also possible. Thus, the XPS data support the successful modification of CNF electrodes with the MB-NiAm complex.

The EDAX analysis of the chemical composition at the surface of CNF electrodes (Table S1, SI) further confirms the successful modification of the electrodes with the MB-NiAm as it shows the presence of Ni (1.4 at.%), concomitantly with a decrease in the atomic percentage of C and a higher percentage of O compared with CNF electrodes and electrodes modified with Meldola Blue.

Additionally, the successful functionalization of CNF electrodes with MB-NiAm is unambiguously confirmed by electrochemistry. Cyclic voltammetry (CV) tests recorded from 0.1 to 0.7 V vs Ag/AgCl in 0.1 M NaOH emphasized a redox couple with an oxidation peak at around + 0.52 V (Fig. 2d) and a reduction peak at + 0.33 V. The anodic peak was attributed to the oxidation of Ni^{2+} to Ni^{3+}, based on the comparison with voltammograms recorded with DRP110 Ni electrodes (carbon electrodes modified with nickel oxide, commercially available), where the electrooxidation of NiO in alkaline media produces nickel oxyhydroxide (NiOOH) [23]. Moreover, the anodic peak at + 0.52 V was not observed with CNF electrodes modified only with MB (Fig. 3d). It is well known that

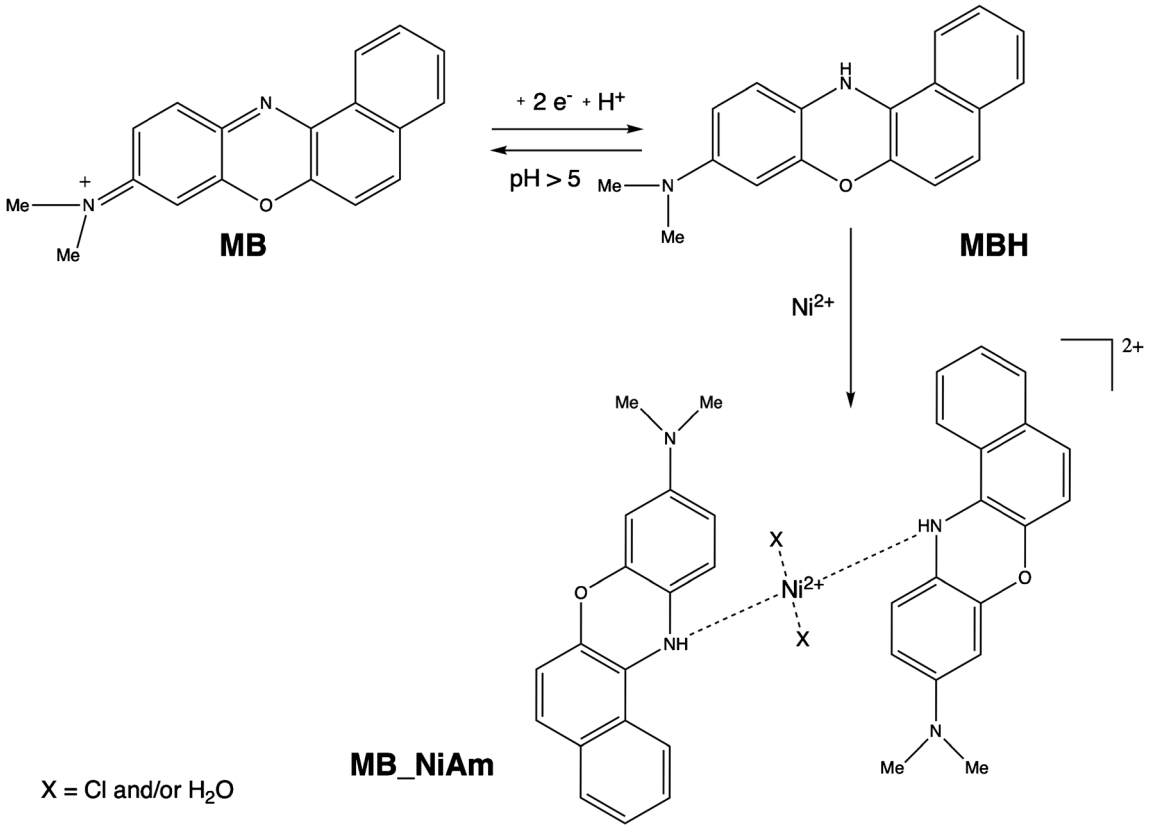

Fig. 1 Schematic representation of the tentative structure of MB-NiAm obtained from the reaction of MB and NiAm

Ni^{3+} is a catalyst for the oxidation of glucose [24]. The presence of Ni^{2+} in CNF/MB-NiAm and the formation of Ni^{3+} in alkaline media were finally confirmed by the electrocatalytic effect of MB-NiAm for the oxidation of glucose (Fig. S4, Supplementary information).

Taken together, the series of microscopy, spectroscopy, and electrochemical studies presented above confirm that a new compound is formed through the reaction of MB with NiAm and that the MB-NiAm compound was successfully transferred onto CNF electrodes.

Performance of NADH sensor based on CNF and CNF/MB-NiAm electrodes

Electrochemical detection of NADH

Cyclic voltammograms recorded using CNF/MB-NiAm electrodes in the − 0.9 to + 0.4 V vs. Ag/AgCl potential range (Fig. 3a) emphasize 3 redox couples with formal potentials of − 0.121 V, − 0.426 V, and − 0.599 V at pH 7.2, similar to electrodes modified with MB only [4]. The formal potential of the redox couples I–III shifts to lower values upon the increase in pH, suggesting that protons are exchanged in the respective transformations. The formal potential of the redox couple I varied in the pH range from 7.2 to 10.1 according to the equation $E^{0'} = -0.039\text{pH} + 0.145$ ($R^2 = 0.989$). The slope of 0.039 V/pH is consistent with one proton and two electrons being transferred in the transformation. Due to the partial overlapping of the peaks II and III, accurate evaluation of the effect of pH on their redox potential was not possible.

Redox couple I of MB with a formal potential of − 0.121 V at pH 7.2 on CNF/MB-NiAm electrode is characteristic of MB and responsible for the mediated electrocatalysis of NADH oxidation. Notably, the mediator enables a 0.5V decrease in overpotential compared with the direct oxidation of NADH on the same CNF electrodes occurring at 0.407 V [4]. Additional redox couples of MB have been reported in the literature for the mediator adsorbed on ordered mesoporous carbon [6] and CNF-modified electrodes [4], as well as for screen-printed carbon electrodes coated with electropolymerized MB [15]. Based on literature data, the redox couples II and III in Fig. 3a are attributed to the mediator bound to oxygen-containing groups on the surface of the electrode. Similar to the other reports where 2 redox couples were observed, only redox couple I is active toward catalysis of NADH oxidation, as shown by the CV in the presence of 10 mmol L^{-1} NADH (Fig. 3b). A steep increase in the anodic current starting at potential values higher than − 0.15 V vs. Ag/AgCl is accompanied by a decrease in the cathodic current at − 0.2 V, the potential corresponding to the reduction peak of redox couple I of the

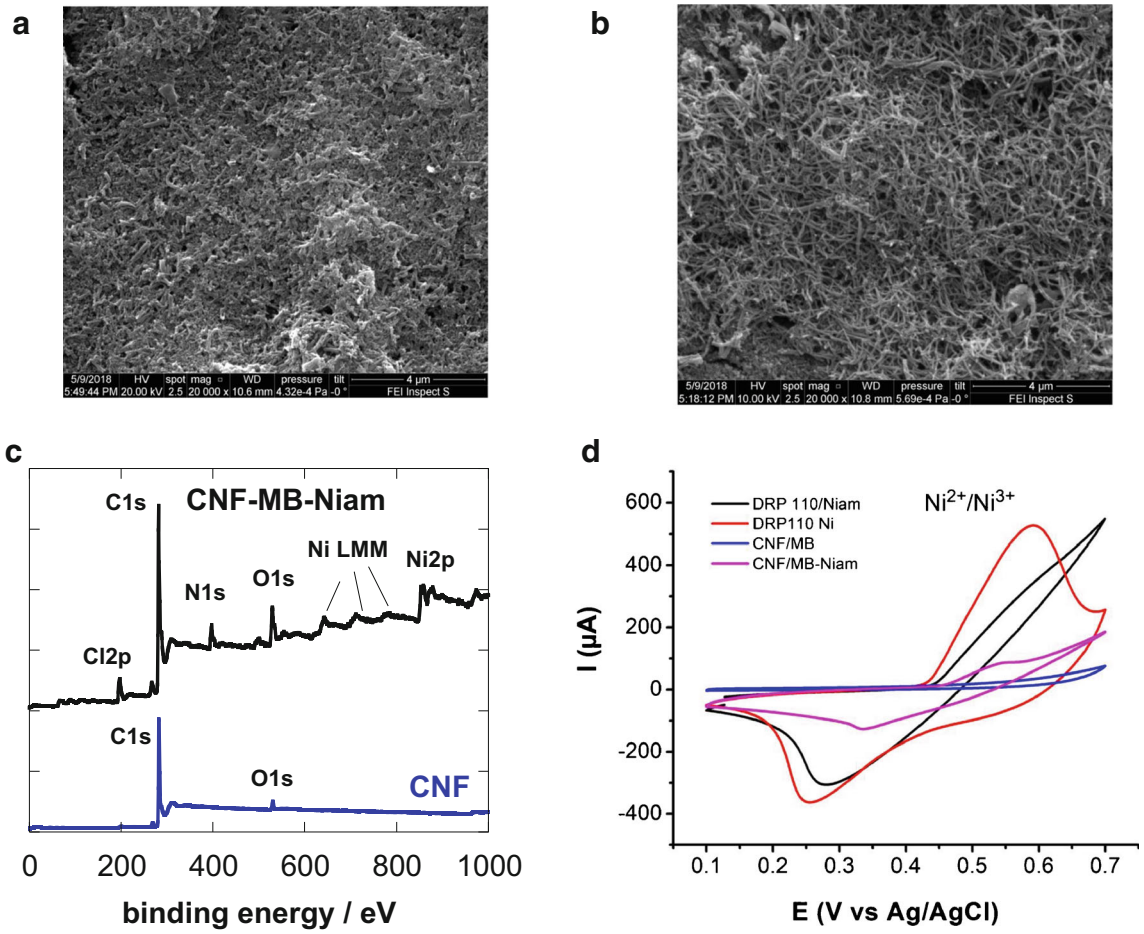

Fig. 2 SEM images obtained at high magnification (× 20,000) of screen-printed carbon nanofiber electrode before (**a**) and after (**b**) modification with drop-casted MB-NiAm. Scale bar: 4 μm. (**c**) XPS survey spectra of carbon nanofiber electrodes before (blue curve) and after (black curve) the modification with MB-NiAm. (**d**) Cyclic voltammograms in 0.1 M NaOH recorded with commercial DRP 110 Ni electrodes, carbon electrodes DRP 110 with drop-casted NiAm, CNF/MB and CNF/MB-NiAm electrodes at 0.1 V/s in the range from 0.1 to 0.7 V

mediator. The catalytic current is attributed to the following sequence of transformations:

$$MB^{+} + NADH \rightarrow MBH + NAD^{+} \quad (2)$$

$$MBH \overset{E>E^{0'}}{\rightarrow} MB + 2e^{-} + H^{+} \quad (3)$$

To determine whether Ni in MB-NiAm is involved in NADH catalysis, we have performed CV studies in the absence and presence of NADH. In parallel, we carried out the same tests with commercial carbon electrodes modified with nickel oxide (DRP 110 Ni). To ensure the formation of NiOOH, which reportedly has catalytic effects toward the oxidation of NADH [23], we have pre-activated both types of electrodes by cyclic voltammetry in 0.1 M NaOH. We did not observe any significant effect of Ni in the electrocatalysis of NADH oxidation mediated by MB-NiAm in 0.1 mol L^{-1} phosphate buffer pH 7.4 (Fig. S5 in SI), thus confirming that the electrocatalytic effect of MB-NiAm is due to the redox couple I of MB.

The performance of the CNF/MB-NiAm electrodes was assessed in PBS buffer (pH 7.4) at + 0.05 V vs. Ag/AgCl in a FIA setup (Fig. 3c). The results feature a detection limit of 0.5 μmol L^{-1} NADH, a linear range that extends to 400 μmol L^{-1} and a sensitivity of 8.9 mA mol^{-1} L (69.8 $mAcm^{-2}$ mol^{-1} L), determined as the slope of the calibration plot (Fig. 3d). A gradual decrease in the performance of CNF/MB-NiAm electrodes was observed at higher pH values, the sensitivity at pH 10 being only 54% of the value at pH 7.4.

The reported detection limit is better than that obtained for electrodes modified with MB by (i) inclusion in the screen-printing ink, either before [10] or after complexation with Reinecke salt [25]; (ii) adsorption on phosphates followed by electrochemical deposition of a Reineckate film [26]; (iii) electropolymerization of Meldola Blue [15] or (iv) inclusion of the mediator in sol-gel after adsorption on single-walled carbon nanotubes [5]. Electrodes modified with CNF and other carbon nanomaterials were successfully used for NADH detection without any mediator, achieving detection limits

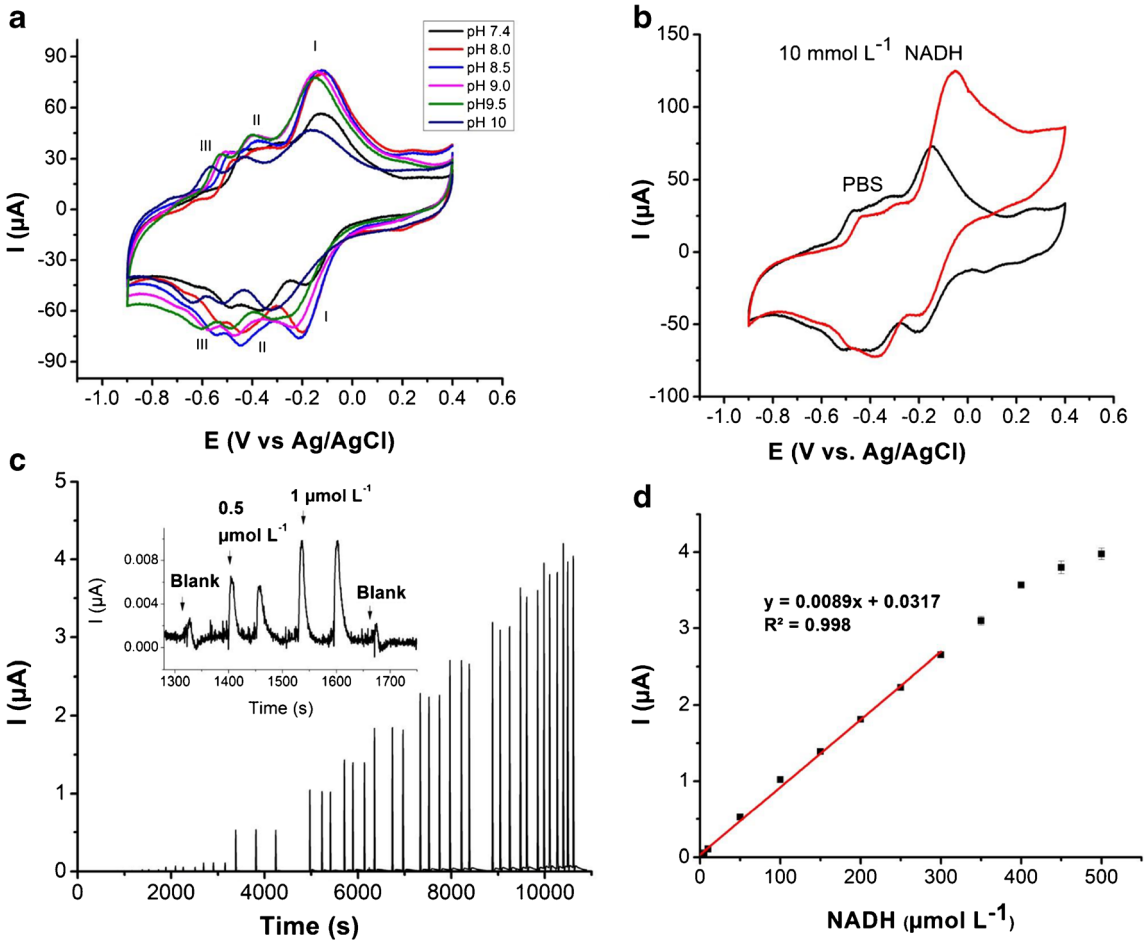

Fig. 3 (**a**) Cyclic voltammograms recorded using CNF/MB-NiAm electrode in solutions of different pH (7.4–10). (**b**) CV recorded in the absence (black) and the presence (red) of 10 mmol L^{-1} NADH in 0.1 mol L^{-1} phosphate buffer pH 7.4. (**c**) Calibration curve for NADH using CNF/MB-NiAm sensor in a FIA setup, at 0.05 V vs. Ag/AgCl, showing (**d**) the linear range

between 0.02 and 130 μmol L^{-1} (Table S2 in SI). However, the sensitivity of these modified electrodes was lower compared with CNF/MB-NiAm electrodes and the applied potential was around + 0.4 V, which makes the measurements susceptible to interferences in real samples (Table S2 in SI). Amperometric NADH sensors with better sensitivity than the CNF/MB-NiAm electrodes but with a narrower linear range have been reported based on rosmarinic acid as mediator [27]. Overall, considering the combined limit of detection, linear range, and sensitivity compared with other sensors described in the literature summarized in Table S2, the novel CNF/MB-NiAm electrodes have good analytical performance as sensitive NADH sensors operating at low potentials.

Stability of MB-NiAm sensors

Cyclic voltammetry studies of MB-NiAm electrodes at different scan rates (0.01 to 0.2 V/s) emphasized a linear correlation between the intensity of the anodic and cathodic peak currents of redox couple I with the scan rate (Fig. S6, SI). This behavior is characteristic for surface-immobilized redox species and together with the lower solubility of the MB-NiAm complex suggests an increased operational stability for NADH detection compared with sensors modified with MB alone.

We have investigated the operational stability in 2 ways: (i) by performing repetitive calibrations by amperometry in stirred solutions and (ii) by repetitive injections of solutions with the same concentration of NADH in a FIA setup. Both types of studies were conducted at + 0.05 V vs. Ag/AgCl in 0.1 M phosphate buffer (pH 7.4). In stirred solutions, the sensitivity decreased from 10 ± 2.4 mA mol^{-1} (average of $n = 3$ sensors) to 9.0 ± 1.4 mA mol^{-1}, i.e., 91.7 ± 7.8% of the initial value after 10 calibrations in the 10–165 μmol L^{-1} range, totaling 80 injections performed on the same day with the same sensor. This compares favorably with CNF/MB-based sensors previously investigated by us, for which the slope of the calibration curve decreased to 70.0 ± 6.2% of the initial value after 10 calibrations [4]. When tested in a FIA setup, the signal for 100 μmol L^{-1} NADH was stable for 100 injections with an RSD of 8.4%. This indicates a very good stability and reproducibility, similar to sensors modified with MB and covered with an electrodeposited Reineckate film reported by Radoi

et al. [26]. For another FIA sensor with MB-Reinecke salt complex, Schuhmann et al. reported a decrease by 40% of the original signal after 60 h of continuous operation totaling 360 injections [13]. The good operational stability indicates that CNF/MB-NiAm sensors are appropriate for use as detectors in biosensors for the high-throughput analysis of dehydrogenase substrates by FIA.

Optimization of the CNF/MB-NiAm/F-ALDH biosensor

A biosensor for the detection of benzaldehyde was obtained by the covalent immobilization of F-ALDH on the CNF/MB-NiAm electrode by cross-linking with glutaraldehyde in an inert matrix of BSA [28]. The biosensor principle lies in benzaldehyde conversion to benzoic acid (catalyzed by F-ALDH) and the measurement of the NADH formed in the enzymatic reaction (1). The biosensor and the operational conditions were optimized with respect to buffer composition and pH, amount of enzyme immobilized on the electrode, concentration of cofactor NAD^+, and the value of the applied potential. The magnitude of the sensor response for a concentration of benzaldehyde of 200 μmol L^{-1} was taken as a criterion for the optimization studies. The range of conditions investigated and the results obtained are detailed in Table S3 and Fig. S7 in the SI. Under optimized conditions, the electrolyte in the FIA system consists of 0.1 M phosphate buffer (pH 10), circulating at a flow rate of 0.33 mL min^{-1}; the enzyme loading/biosensor is 36 mU; the NAD^+ concentration is 1.75 mmol L^{-1}; and the applied potential is + 0.1 V vs Ag/AgCl.

Selectivity and stability of the CNF/MB-NiAm/F-ALDH biosensor

The selectivity of the biosensor is mainly given by (i) the substrate selectivity of the enzyme and (ii) the value of the applied potential. The MB-NiAm mediator enables the efficient operation of the biosensor at close to 0 V, ensuring minimized electrochemical interferences. F-ALDH has broad substrate specificity for aldehydes, while being inactive toward compounds from other chemical classes. This broad selectivity is a characteristic of aldehyde dehydrogenases from different sources, including the commercial enzyme from yeast used in other aldehyde biosensors [16, 25, 28, 29]. As anticipated, the biosensor responded well to a series of aromatic and aliphatic aldehydes, tested at the concentration of 200 μmol L^{-1} (Fig. 4) and was insensitive to compounds from chemical classes other than aldehydes, i.e., benzoic acid, benzyl alcohol, acetic acid, acetone, and ethanol, tested at concentrations relevant for real samples such as benzyl alcohol and wine. Benzaldehyde is among the aldehydes for which F-ALDH has high activity, the largest response being recorded for isovaleraldehyde. The results are in agreement with UV-vis measurements of enzyme activity performed with the free enzyme in solution (unpublished data). Benzaldehyde determination was previously demonstrated by Badalyan et al. [18] with an amperometric biosensor based on the PaoABC-aldehyde oxidoreductase from *E. coli*, which has a preference for aromatic aldehydes and a $K_M = 70$ μmol L^{-1} for benzaldehyde.

Detection of a specific aldehyde in an aldehyde mixture with the CNF/MB-NiAm/F-ALDH biosensor might not be possible or additional steps should be included to ensure selectivity such as use of sensor arrays [30] instead of a single biosensor, detection in air at different temperatures, and addition of diffusion-limiting membranes. Thus, a biosensor based on F-ALDH is mostly useful to detect a particular aldehyde when this is the major or only aldehyde in a sample, e.g., the detection of benzaldehyde in benzyl alcohol or the detection of acetaldehyde in wine. In this work, similar to the study of Badalyan et al. [18], we chose to investigate the performances of the biosensor for the analysis of benzyl alcohol, where benzaldehyde is present as a major impurity while other aldehydes are not expected.

The operational stability of the biosensor was checked by injecting solutions of 300 μmol L^{-1} benzaldehyde over the course of 4 days. The biosensor was operated at room temperature. During the night, the biosensor was dismounted from the flow cell and stored dry in the fridge until the next day. With over 60 repetitive daily injections of 300 μmol L^{-1} benzaldehyde, the biosensor response varied very little (RSD of 5.6–7.5%). However, a significant drop in sensitivity was recorded from one day to the next: the magnitude of the current dropped to 73.7% from the initial value after 1 day, 53.3% after 2 days, and 43.3% in the 4^{th} day. With daily calibration, the biosensor might be used for at least 3 days of extensive testing. Moreover, optimizing the overnight storage might further prolong the operational lifetime of the biosensor.

Based on the magnitude of the signal for 200 μmol L^{-1} benzaldehyde, the biosensor retains 91.1% of the original activity after 40 days when kept dry at 4 °C (0.270 ± 0.087 μA compared with 0.297 ± 0.037 μA initially, for $n = 3$ injections).

Performance for the detection of benzaldehyde

Calibration curves performed for benzaldehyde by amperometry at + 0.1 V in the range up to 500 μmol L^{-1} highlight a detection limit of 10 μmol L^{-1}, a linear range of 30–300 μmol L^{-1}, and a sensitivity of 1.1 mA mol^{-1} L or 8.73 mA cm^{-2} mol^{-1} 1 L (Fig. 5).

The detection limit calculated as three times the signal of the blank (i.e., running buffer containing NAD^+) was verified experimentally (Fig. S8 in SI). In addition, it was checked that the biosensor does not present any memory effect (Fig. S9 in SI).

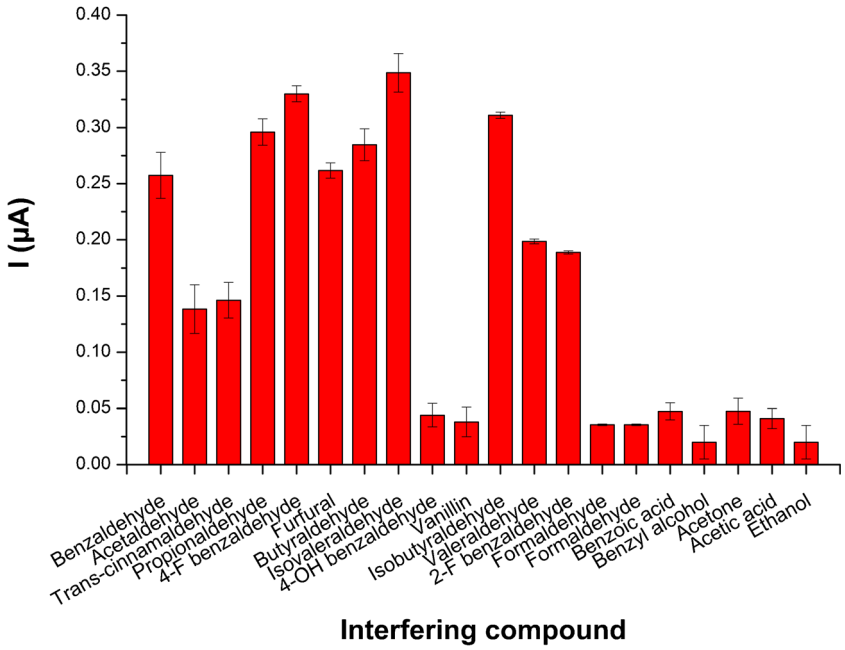

Fig. 4 Selectivity of CNF/MB-NiAm/F-ALDH biosensor: magnitude of the current intensity recorded with the biosensor for 200 μmol L^{-1} solutions of various aldehydes in the presence of 3.2 mmol L^{-1} NAD^+, measured at + 0.1 V vs Ag/AgCl in 0.1 M phosphate buffer (pH 10) with 0.1 M KCl. Also included are benzoic acid (1 mmol L^{-1}), benzyl alcohol (diluted 1:50 with buffer), acetone (200 μmol L^{-1}), acetic acid (2 mmol L^{-1}), and ethanol (0.12%)

Biosensor reproducibility is acceptable, considering the manual modification step: an RSD of 8.84% was determined for the sensitivity of three identically prepared and tested biosensors, expressed as the slope of the calibration curve based on 5 concentrations of benzaldehyde in the range 30–300 μmol L^{-1}.

The kinetic parameters of the immobilized enzyme in the CNF/MB-NiAm/F-ALDH biosensor were calculated from the plots of the amperometric signal *versus* benzaldehyde concentration. Data was fitted with the hyperbolic function $I=I_{max}*c/(K_M^{app}+c)$ using Origin 2019 software, where I_{max} represents the maximum current intensity recorded with the biosensor, K_M^{app} is the apparent Michaelis-Menten constant of the immobilized F-ALDH in the biosensor, and c is the concentration of benzaldehyde. The K_M^{app} for the immobilized enzyme was calculated as 386 μmol L^{-1} and the I_{max} was 0.590 μA. The Michaelis constant is higher than the value for the free enzyme (K_M = 145 μmol L^{-1}), which is attributed both to diffusional limitations for substrate and cofactor to the catalytic site of the enzyme and to conformational changes of the immobilized enzyme that lead to a decreased affinity for the substrate.

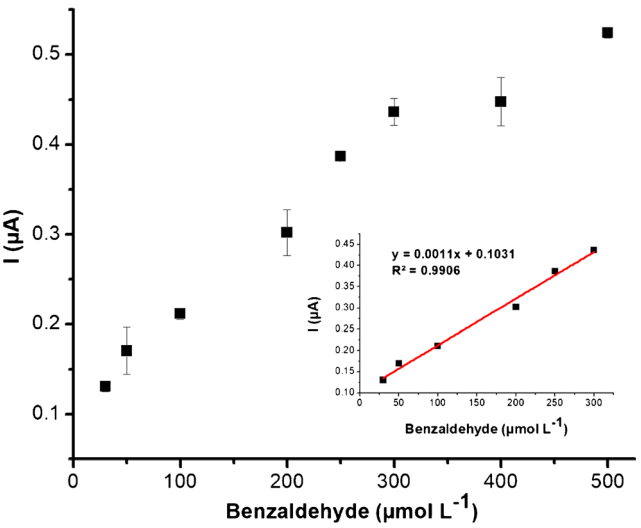

Fig. 5 Calibration plot for benzaldehyde using the CNF/MB-NiAm/F-ALDH biosensor in a FIA system at + 0.1 V vs. Ag/AgCl in 0.1 M phosphate buffer pH 10 with 0.1 M KCl and 10 μM β-mercaptoethanol (added to ensure the stability of the enzyme)

Cross-linking with glutaraldehyde in an inert matrix of BSA is widely used to achieve stable immobilization of enzymes [31] and typically leads to an increased K_M: for example, covalent attachment by this method of aldehyde dehydrogenase from baker's yeast with K_M = 53 μM [32] to a Nylon mesh enabled to obtain an amperometric biosensor with a K_M^{app} = 550 μM for benzaldehyde [28]. Optimization of the immobilization protocol or alternative methods to attach the enzyme on the electrode can lead in the future to improved affinity of the immobilized F-ALDH enzyme for benzaldehyde.

Overall, the analytical performances of the biosensor are similar with those of other enzymatic sensors for aldehydes. While other biosensors for benzaldehyde, formaldehyde, or acetaldehyde have broader linear ranges or better detection limits (Table S4, SI), down to 0.5 μmol L^{-1} [18] for some of them, the high sensitivities are achieved with bienzymatic systems, implying higher costs and complexity of the assay [16]. Some simpler nanomaterial-based electrochemical methods report pmol L^{-1} detection limits for benzaldehyde [33]; however, no data is available on their reusability and response to a whole range of other aldehydes. The CNF/

MB-NiAm/F-ALDH biosensor responds to lower aldehyde concentrations compared with some optical methods involving sensor arrays; nonetheless, these arrays combined with chemometric analysis can discriminate between several aldehydes [30]. Along with better detection limit and shorter analysis time (5 min/analysis compared with 10 min/assay), sensor reusability and stability are the main advances of the proposed CNF/MB-NiAm/F-ALDH sensor over our previous assay for benzaldehyde that was based on free F-ALDH in solution and CNF electrodes with Meldola Blue and electrochemically reduced graphene oxide [4]. The need for the enzymatic cofactor was addressed in different ways in the biosensors for aldehydes (Table S4, SI). Ingenious, reagentless biosensors integrate either enzymes with bound cofactor such as PaoABC-aldehyde oxidoreductase from *E. coli* [18] or immobilized, costly high molecular weight derivatives of NAD^+ [29]. In the setup proposed in this work, NAD^+ is added only to the sample (and not to the running buffer), thus limiting the amount and costs of the enzymatic cofactor compared with other FIA [34] and batch determinations in stirred solutions [5, 6]. Moreover, the amount of enzyme per CNF/MB-NiAm/F-ALDH biosensor compares favorably with other sensors and allows performing > 160 assays with the same device. In summary, depending on the envisaged application, the described biosensor with its good analytical characteristics and operational stability is advantageous over other chemical or enzyme sensors.

Detection of benzaldehyde in benzyl alcohol and comparison with HPLC

Benzyl alcohol is used in the pharmaceutical industry as a preservative for liquid dose drugs (i.e., ophthalmic, otic solutions, etc.). The quantitative detection of benzaldehyde as a major impurity in benzyl alcohol is important for the quality control of this pharmaceutical excipient. Therefore, we have examined the usefulness of the CNF/MB-NiAm/F-ALDH biosensor for this application.

A series of benzyl alcohol samples, unspiked and spiked with benzaldehyde, were analyzed in parallel with the CNF/MB-NiAm/F-ALDH biosensor and by HPLC. Benzaldehyde was not detected in the unspiked benzyl alcohol by either methods (Table 1). The results summarized in Table 1 emphasize the agreement between the two methods, indicating the high accuracy of the biosensor. Moreover, the recovery factors for benzaldehyde calculated as "the determined concentration/spiked concentration x100" were in the ranges of 90.8–106.5% for the biosensor and 97.1–108.2% for the HPLC method. Altogether, the biosensor is appropriate for determining benzaldehyde in benzyl alcohol for non-parenteral use, for which a maximum admissible limit of 0.15% (14.4 mmol L^{-1}) is currently imposed [19].

The biosensor described here provides a simple alternative tool to the lengthier and costlier chromatographic procedures for the quality control of benzyl alcohol [19], being also faster and simpler compared with sandwich ELISA [35] or SPR immunosensors [36].

Conclusion

A new, low-solubility, versatile mediator was obtained from Meldola Blue and a Ni amine, preserving the characteristics of both Meldola Blue and Ni^{2+}. The new compound efficiently catalyzes NADH electrochemical oxidation at a similar potential as Meldola Blue. While not further pursued, it was shown that the presence of Ni^{2+} in the mediator enables also the electrocatalysis of glucose oxidation in alkaline media. Modification of CNF screen-printed electrodes with the low-solubility MB-NiAm complex resulted in stable and sensitive amperometric NADH sensors operating at low potentials. Further on, integration of an aldehyde dehydrogenase from a microorganism from Antarctica covalently immobilized on the electrode surface produced stable biosensors for the detection of aldehydes. Detection of benzaldehyde in the μmol L^{-1} range was demonstrated with the biosensor in a flow injection setup. Due to the characteristics of the aldehyde dehydrogenase used, the biosensor has a broad selectivity profile responding to various aldehydes, although not to other classes of volatile organic compounds. Consequently, the potential of the new biosensor is best exploited in situations where a single

Table 1 Analysis of benzaldehyde in spiked benzyl alcohol samples with CNF/MB-NiAm/F-ALDH biosensor and HPLC

Sample	Spiked concentration, benzaldehyde (mmol L^{-1})	Concentration determined with the biosensor ($n = 3$) (mmol L^{-1})	Recovery (%) Biosensor	Benzaldehyde concentration measured by HPLC (mmol L^{-1})	Recovery (%) HPLC
Benzyl alcohol	0	< 0.50*	Not applicable	< 0.35*	Not applicable
Benzyl alcohol	9	8.17 ± 0.73	90.8 ± 8.1	8.74 ± 0.24	97.1 ± 2.7
Benzyl alcohol	24	25.47 ± 3.01	106.1 ± 12.5	25.97 ± 0.92	108.2 ± 3.8
Benzyl alcohol	47	49.09 ± 8.85	104.4 ± 18.8	50.80 ± 0.17	108.1 ± 0.4

*Based on the detection limit of the method and the dilution factor

aldehyde is present or when the aldehyde represents the majority in a mixture of volatile organic compounds. Such an application of industrial relevance was illustrated through the detection of benzaldehyde in benzyl alcohol, used as an inactive ingredient in liquid drug products. The biosensor accuracy was validated by comparison with a standard chromatographic method, indicating that this new analytical device can be successfully used for the quality control of benzyl alcohol. While the amount of NAD^+ per test was minimized by adding the cofactor together with the sample in the injection loop of the FIA system, the addition of NAD^+ is still required for each test. Future tests will tackle the challenge of stable cofactor immobilization. More importantly, while the measurements described in this work were conducted at room temperature, the potential of the psychrophilic F-ALDH enzyme remains to be fully exploited in future works by developing biosensors performing at low temperature.

Acknowledgments The authors wish to thank Medana Zamfir, Institute of Biology of the Romanian Academy, for the support with HPLC measurements.

Funding information This study was financially supported by the Romanian Executive Agency for Higher Education, Research, Development and Innovation (UEFISCDI), through PN-III-P2-2.1-PED-2016-0116 grant and ERANET-M-ENZ4IFACES contract 166/01.05.2020 for Ana Maria Titoiu, Georgiana Necula-Petrareanu, Cristina Purcarea and Alina Vasilescu.

Compliance with ethical standards

Conflict of interest The authors declare that they have no competing interests.

References

1. Fanjul-Bolado P, Queipo P, Lamas-Ardisana PJ, Costa-García A (2007) Manufacture and evaluation of carbon nanotube modified screen-printed electrodes as electrochemical tools. Talanta 74(3):427–433. https://doi.org/10.1016/j.talanta.2007.07.035
2. Huang J, Liu Y, You T (2010) Carbon nanofiber based electrochemical biosensors: a review. Anal Methods 2(3):202–211. https://doi.org/10.1039/B9AY00312F
3. Wang Z, Wu S, Wang J, Yu A, Wei G (2019) Carbon nanofiber-based functional nanomaterials for sensor applications. Nanomaterials (Basel, Switzerland) 9(7). https://doi.org/10.3390/nano9071045
4. Titoiu AM, Lapauw M, Necula-Petrareanu G, Purcarea C, Fanjul-Bolado P, Marty J-L, Vasilescu A (2018) Carbon nanofiber and Meldola Blue based electrochemical sensor for NADH: application to the detection of benzaldehyde. Electroanalysis 30(11):2676–2688. https://doi.org/10.1002/elan.201800472
5. Arvinte A, Sesay Adama M, Virtanen V, Bala C (2008) Evaluation of Meldola Blue-carbon nanotube-sol-gel composite for electrochemical NADH sensors and their application for lactate dehydrogenase-based biosensors. Electroanalysis 20(21):2355–2362. https://doi.org/10.1002/elan.200804332
6. Jiang X, Zhu L, Yang D, Mao X, Wu Y (2009) Amperometric ethanol biosensor based on integration of alcohol dehydrogenase with Meldola's Blue/ordered mesoporous carbon electrode. Electroanalysis 21(14):1617–1623. https://doi.org/10.1002/elan.200804586
7. Gorton L, Domínguez E (2002) Electrocatalytic oxidation of NAD(P)/H at mediator-modified electrodes. Rev Mol Biotechnol 82(4):371–392. https://doi.org/10.1016/S1389-0352(01)00053-8
8. Santhiago M, Strauss M, Pereira MP, Chagas AS, Bufon CCB (2017) Direct drawing method of graphite onto paper for high-performance flexible electrochemical sensors. ACS Appl Mater Interfaces 9(13):11959–11966. https://doi.org/10.1021/acsami.6b15646
9. Munteanu FD, Kubota LT, Gorton L (2001) Effect of pH on the catalytic electrooxidation of NADH using different two-electron mediators immobilised on zirconium phosphate. J Electroanal Chem 509(1):2–10. https://doi.org/10.1016/S0022-0728(01)00376-X
10. Sprules SD, Hart JP, Wring SA, Pittson R (1994) Development of a disposable amperometric sensor for reduced nicotinamide adenine dinucleotide based on a chemically modified screen-printed carbon electrode. Analyst 119(2):253–257. https://doi.org/10.1039/AN9941900253
11. Taniguchi I, Shimoota T, Tominaga M, Nishiyama K (1994) Potential-dependent rectified electron transfer at a Meldola's Blue incorporated decanethiol-modified electrode as a model of biological membrane. Microchem J 49(2):340–354. https://doi.org/10.1006/mchj.1994.1045
12. Doaga R, McCormac T, Dempsey E (2009) Electrochemical sensing of NADH and glutamate based on Meldola Blue in 1,2-diaminobenzene and 3,4-ethylenedioxythiophene polymer films. Electroanalysis 21(19):2099–2108. https://doi.org/10.1002/elan.200904627
13. Schuhmann W, Huber J, Wohlschläger H, Strehlitz B, Gründig B (1993) Electrocatalytic oxidation of NADH at mediator-modified electrode surfaces. J Biotechnol 27(2):129–142. https://doi.org/10.1016/0168-1656(93)90103-T
14. Kumar SA, Chen SM (2007) Fabrication and characterization of Meldola's Blue/zinc oxide hybrid electrodes for efficient detection of the reduced form of nicotinamide adenine dinucleotide at low potential. Anal Chim Acta 592(1):36–44. https://doi.org/10.1016/j.aca.2007.04.022
15. Vasilescu A, Andreescu S, Bala C, Litescu SC, Noguer T, Marty J-L (2003) Screen-printed electrodes with electropolymerized Meldola Blue as versatile detectors in biosensors. Biosens Bioelectron 18(5):781–790. https://doi.org/10.1016/S0956-5663(03)00044-7
16. Ghica ME, Pauliukaite R, Marchand N, Devic E, Brett CM (2007) An improved biosensor for acetaldehyde determination using a bienzymatic strategy at poly(neutral red) modified carbon film electrodes. Anal Chim Acta 591(1):80–86. https://doi.org/10.1016/j.aca.2007.03.047
17. Mitsubayashi K, Nishio G, Sawai M, Kazawa E, Yoshida H, Saito T, Kudo H, Otsuka K, Takao M, Saito H (2008) A biochemical sniffer-chip for convenient analysis of gaseous formaldehyde from timber materials. Microchim Acta 160(4):427–433. https://doi.org/10.1007/s00604-007-0799-7
18. Badalyan A, Neumann-Schaal M, Leimkühler S, Wollenberger U (2013) A biosensor for aromatic aldehydes comprising the mediator dependent PaoABC-aldehyde oxidoreductase. Electroanalysis 25(1):101–108. https://doi.org/10.1002/elan.201200362
19. European Council, European Directorate for the Quality of Medicines and Healthcare (2019) Benzyl alcohol monograph. European Pharmacopoeia 94:5327–5327
20. Necula-Petrareanu G, Lavin P, Vasilescu A, Purcarea C (2018) Antarctic Flavobacterium aldehyde dehydrogenase – a cold-

adapted catalyst for biosensing. J Biotechnol 280:S18. https://doi.org/10.1016/j.jbiotec.2018.06.054
21. King HJS, Cruse AW, Angell FG (1932) 448. Researches on ammines. Part VI. Nickelammine salts in aqueous solution. Journal of the Chemical Society (Resumed) (0):2928-2931. https://doi.org/10.1039/JR9320002928
22. Mažeikienė R, Niaura G, Eicher-Lorka O, Malinauskas A (2011) Raman spectroelectrochemical study of Meldola Blue, adsorbed and electropolymerized at a gold electrode. J Colloid Interface Sci 357(1):189–197. https://doi.org/10.1016/j.jcis.2011.01.086
23. Hassan KM, Hathoot AA, Ashour WFD, Abdel-Azzem M (2015) Electrochemical and analytical applications for NADH detection at glassy carbon electrode modified with nickel nanoparticles dispersed on poly 1,5-diaminonaphthalene. J Solid State Electrochem 19(4):1063–1072. https://doi.org/10.1007/s10008-014-2705-7
24. Hou L, Bi S, Lan B, Zhao H, Zhu L, Xu Y, Lu Y (2019) A novel and ultrasensitive nonenzymatic glucose sensor based on pulsed laser scribed carbon paper decorated with nanoporous nickel network. Anal Chim Acta 1082:165–175. https://doi.org/10.1016/j.aca.2019.07.056
25. Avramescu A, Noguer T, Avramescu M, Marty J-L (2002) Screen-printed biosensors for the control of wine quality based on lactate and acetaldehyde determination. Anal Chim Acta 458(1):203–213. https://doi.org/10.1016/S0003-2670(01)01580-X
26. Radoi A, Compagnone D, Batic M, Klincar J, Gorton L, Palleschi G (2007) NADH screen-printed electrodes modified with zirconium phosphate, Meldola blue, and Reinecke salt. Application to the detection of glycerol by FIA. Anal Bioanal Chem 387(3):1049–1058. https://doi.org/10.1007/s00216-006-0975-3
27. Bilgi M, Sahin EM, Ayranci E (2018) Sensor and biosensor application of a new redox mediator: rosmarinic acid modified screen-printed carbon electrode for electrochemical determination of NADH and ethanol. J Electroanal Chem 813:67–74. https://doi.org/10.1016/j.jelechem.2018.02.012
28. Pariente F, Lorenzo E, Tobalina F, Abruna HD (1995) Aldehyde biosensor based on the determination of NADH enzymically generated by aldehyde dehydrogenase. Anal Chem 67(21):3936–3944. https://doi.org/10.1021/ac00117a019
29. Noguer T, Marty JL (1997) Reagentless sensors for acetaldehyde. Anal Lett 30(6):1069–1080. https://doi.org/10.1080/00032719708004039
30. Li Y, Liu X, Wu Q, Yi J, Zhang G (2018) Discrimination and detection of benzaldehyde derivatives using sensor array based on fluorescent carbon nanodots. Sensors Actuators B Chem 261:271–278. https://doi.org/10.1016/j.snb.2018.01.160
31. Nguyen HH, Lee SH, Lee UJ, Fermin CD, Kim M (2019) Immobilized enzymes in biosensor applications. Materials (Basel, Switzerland) 12(1). https://doi.org/10.3390/ma12010121
32. Bradbury SL, Clark JF, Steinman CR, Jakoby WB (1975) Aldehyde dehydrogenase from baker's yeast. Methods Enzymol 41:354–360. https://doi.org/10.1016/s0076-6879(75)41079-5
33. Subhan MA, Chandra SP, Sumon S, Ahmed J, Asiri AM, Rahman M, Al-Mamun M (2018) Enhanced photocatalytic activity and ultra-sensitive benzaldehyde sensing performances of SnO2•ZnO•TiO2 nanomaterials. RSC Adv 8:33048–33058. https://doi.org/10.1039/C8RA05182H
34. Premaratne G, Farias S, Krishnan S (2017) Pyrenyl carbon nanostructures for ultrasensitive measurements of formaldehyde in urine. Anal Chim Acta 970:23–29. https://doi.org/10.1016/j.aca.2017.03.032
35. Shirasu N, Onodera T, Nagatomo K, Shimohigashi Y, Toko K, Matsumoto K (2009) Noncompetitive immunodetection of benzaldehyde by open sandwich ELISA. Anal Sci 25(9):1095–1100. https://doi.org/10.2116/analsci.25.1095
36. Onodera T, Shimizu T, Miura N, Matsumoto K, Toko K (2010) Surface plasmon resonance based sensitive immunosensor for benzaldehyde detection. IEEJ Transactions on Sensors and Micromachines 130(7):269–274. https://doi.org/10.1541/ieejsmas.130.269